Generation of 120 GW mid-infrared pulses from a widely tunable noncollinear optical parametric amplifier

Kun Zhao,[1] Haizhe Zhong,[1] Peng Yuan,[2,*] Guoqiang Xie,[2] Jing Wang,[2] Jingui Ma,[1] and Liejia Qian[1]

[1]*Shanghai Engineering Research Center of Ultra-Precision Optical Manufacturing, Department of Optical Science and Engineering, Fudan University, Shanghai 200433, China*

[2]*Key Laboratory for Laser Plasmas (Ministry of Education), Physics Department, Shanghai Jiao Tong University, Shanghai 200240, China*

**Corresponding author: pengyuan@sjtu.edu.cn*

Received April 1, 2013; revised May 18, 2013; accepted May 22, 2013; posted May 23, 2013 (Doc. ID 188000); published June 18, 2013

We demonstrate a noncollinear optical parametric chirped-pulse amplification scheme for generating high-peak-power tunable mid-infrared (IR) pulses. The high-gain $LiNbO_3$-based noncollinear parametric amplifier, seeded by a tunable femtosecond optical parametric amplifier, provides a wide wavelength tuning range from 3.3 to 3.95 μm and a large saturated gain of over 4000 in a single-stage amplifier. The compressed mid-IR pulse has a pulse energy of 13.3 mJ and pulse duration of 111 fs, with a peak power as high as 120 GW. To the best of our knowledge, this is the highest peak power ever reported for 3–5 μm tunable mid-IR lasers.

OCIS codes: (320.7110) Ultrafast nonlinear optics; (190.4970) Parametric oscillators and amplifiers.
http://dx.doi.org/10.1364/OL.38.002159

Mid-infrared (IR) lasers have attracted tremendous interest in medicine, scientific, and military applications. For instance, intense mid-IR ultrafast lasers will be an ideal driver for high-harmonic generation (HHG) [1]. The relationship between the HHG cutoff photon energy E_{cutoff} and the ponderomotive energy U_p of the free electron in the laser field can be described in atomic units by the formula $E_{\mathrm{cutoff}} = I_p + 3.17\ U_p$ ($U_p \approx I_L\lambda^2$), where I_p is the ionization potential of the gas atom and I_L is the intensity of the laser. Thus, driving lasers with longer wavelengths will result in a higher single-atom cutoff photon energy. Moreover, the phase matching (PM) and macroscopic response of the medium in HHG generation are more favorable at longer driving wavelengths, which is essential for achieving significant HHG flux [1,2]. In future applications, the high-flux coherent x ray at the water window band will be a desirable source for medical imaging.

Currently, most of the high-power femtosecond lasers operate at near-infrared (NIR) wavelengths, such as the Ti: sapphire chirped-pulse amplifier (CPA) at 800 nm. However, optical parametric chirped-pulse amplifiers (OPCPAs) have relaxed the restrictions of gain materials and may support high-power ultrashort pulse generation in a wide spectral region [3,4]. With the seeding from available mode-locked femtosecond oscillators such as Ti:sapphire, Nd:glass, and Er:fiber lasers, OPCPAs can support high-power ultrashort pulse generation at NIR wavelengths similar to the previous CPA systems [5–7]. Moreover, with the features of ultrabroad gain bandwidth and a low thermal effect, OPCPAs manifest superiorities for high average power and few-cycle pulse generation [8].

Extensions of OPCPA technology to the mid-IR regime, however, have faced considerable difficulties such as the generation of a mid-IR seed pulse, suitable nonlinear crystals for high parametric gain, etc. So far, mid-IR OPCPA systems have been reported at 2 μm [9,10], 3 μm [11], and 4 μm wavelength [12,13]. In these systems, the mid-IR seed pulses were produced by means of intrapulse difference-frequency generation (DFG) of a few-cycle Ti:sapphire laser [9,10], DFG of two temporally synchronized pulses with different wavelengths [14], and idler seeding from a NIR femtosecond optical parametric amplifier (OPA) [13]. As a consequence of the seeding pulses used, these OPCPA systems show a common difficulty of wavelength tunability. In high-peak-power laser systems using bulk nonlinear crystals, it is also difficult for mid-IR OPCPAs to achieve a high parametric gain similar to that in NIR OPCPAs. Taking the commonly used bulk $KTiOAsO_4$ (KTA) crystal as an example, the parametric gain is usually about 100 or less for mid-IR OPCPAs [7,13,15].

In this Letter, we demonstrate a widely tunable OPCPA system that generates mid-IR femtosecond pulses with the highest peak power of 120 GW so far. Different from previously reported works, the mid-IR OPCPA scheme adopts seeding from a tunable mid-IR femtosecond OPA and noncollinear PM, allowing wavelength tuning from 3.3 to 3.95 μm. By employing a high-gain $LiNbO_3$-based parametric amplifier, we demonstrate a saturated gain of over 4000 in a single-stage amplifier that directly boosts the signal to a chirped-pulse energy of 29.5 mJ. After compression, the mid-IR laser has a pulse energy of 13.3 mJ and pulse duration of 111 fs, with a peak power of 120 GW.

The layout of the mid-IR OPCPA system is shown in Fig. 1. Two laser amplifier systems are used as pump

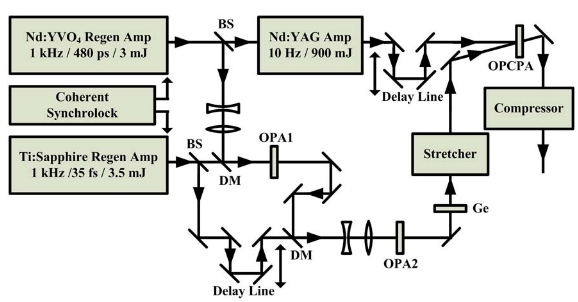

Fig. 1. Layout of the tunable mid-IR OPCPA system. BS, beam splitter; DM, dichroic mirrors for 800 nm and 1 μm; Ge, germanium plate.

sources for the OPCPA: one is a femtosecond Ti:sapphire laser regenerative amplifier (Coherent, Legend Elite) with a pulse energy of 3.5 mJ and pulse duration of 35 fs, and the other is a high-energy long pulse (480 ps) laser system consisting of a 3 mJ Nd:YVO_4 laser regenerative amplifier (High-Q, Pico-Regen) followed by a 10 Hz Nd:YAG boost amplifier (Innolas, SpitLight) with a pulse energy of 900 mJ. The two regenerative amplifiers, both operating at a kilohertz repetition rate, were well synchronized by an electronic phase-locking loop (time jitter ~10 ps). The front end of the OPCPA system consists of a two-stage mid-IR femtosecond OPA pumped by the Ti:sapphire laser. Two 12 mm thick uncoated $LiNbO_3$ crystals (CASTECH) cut at $\theta = 45°$ for type-I collinear PM were used in the first and second OPA stages. In the configuration of collinear PM, $LiNbO_3$ crystals manifest a nearly vanished group-velocity mismatch (GVM) at the idler wavelength of 3425 nm, which is quite suitable to our application. The Ti: sapphire laser acted as a pump for the first (0.6 mJ) and second (2.6 mJ) stage OPA, while a fraction of the Nd:YVO_4 laser output (20%) was used for seeding the first stage OPA. The seeding beam was telescoped up to a diameter of 8.5 mm to collinearly match the femtosecond pump beam in the first stage. The generated femtosecond signal pulses around 1 μm and the pump pulses from the Ti:Sapphire laser output were then combined by a dichroic mirror and directed to the second stage OPA, which was also kept a strictly collinear geometry to avoid angular dispersion of the generated mid-IR pulses. The pump beam of the second stage OPA was designed to a size of 17 mm, corresponding to a laser intensity of ~30 GW/cm^2. Once the pump intensity was beyond 50 GW/cm^2 in the experiment, beam distortions induced by self-focusing were observed, which severely degraded the beam quality of the generated mid-IR laser.

The femtosecond OPA generated mid-IR pulses with a maximum pulse energy of 50 μJ and a wavelength tuning range of 3.3 to 3.95 μm. The generated mid-IR pulses were checked to be free of angular dispersion because of the employed collinear PM, which is desirable for seeding the OPCPA. Figures 2(a)–2(c) show the typical pulse spectra from the OPA at three different wavelengths. We simply discuss why this OPA seeded by the narrowband laser can be tunable. Since the seed pulse energy within the pump duration is only ~50 nJ, the first OPA stage is subject to an amplification regime of weak seeding. In such an OPA with weak seeding, the central wavelength of a generated femtosecond signal pulse is mainly determined by its PM condition, while the narrowband laser just initiates the parametric process as long as the seeding wavelength is located within the gain bandwidth [16]. Thus, the PM wavelength does not necessary have to be exactly identical to the seeding wavelength, and our femtosecond OPA can be tunable in wavelength by adjusting the crystal orientation. For the same reason, the second OPA stage can further enhance the wavelength tunability to some extent. The mid-IR pulse duration output from the second stage OPA were measured to be ~100 to 200 fs depending on their wavelengths, corresponding to ~10 light cycles similar to that of the Ti:sapphire laser.

In the OPCPA system, a single-stage $LiNbO_3$-based noncollinear parametric amplifier was used to amplify the mid-IR pulses. The $LiNbO_3$ crystal employed in the OPCPA was cut at $\theta = 56°$ for type-I PM with a pump-signal crossing angle of ~7.2°. It is worthwhile to note that mid-IR seeding is necessary for a vanishing GVM in the configuration of a noncollinear PM. The 10 Hz Nd:YAG amplifier with a pulse energy of 900 mJ served as the pump laser. Mid-infrared pulses from the second stage femtosecond OPA were temporally stretched to ~430 ps by using a double-pass Öffner stretcher, and the chirped-pulse energy was reduced to 7 μJ or less. Both the pump and seed beams were telescoped to a similar diameter of 11 mm, which resulted in a maximum pump intensity of ~2 GW/cm^2, well below the damage threshold of the $LiNbO_3$ crystal. $LiNbO_3$ was selected as the OPCPA nonlinear crystal because of its relatively large nonlinear coefficient ($d_{\mathrm{eff}} \approx 4$ pm/V), which can theoretically provide a saturated high gain of ~10^4 with a crystal length of 40 mm. In the experiment, the amplified pulse energy was 29.5 mJ at a wavelength of 3425 nm, corresponding to a saturated parametric gain over 4000 and an overall conversion efficiency of ~10% (Fig. 3). By blocking the seeding, we did not observe detectable optical parametric superfluorescence. As a consequence of tunable mid-IR seeding and noncollinear PM, the OPCPA can be tuned from 3.3 to 3.95 μm (Fig. 3) by adjusting the OPCPA crystal, noncolliner angle, and the crystal orientations in seeding stage accordingly. Three typical spectra of amplified mid-IR pulses are given in Figs. 2(d)–2(f). The amplified chirped pulses were compressed by a double-pass grating pair compressor.

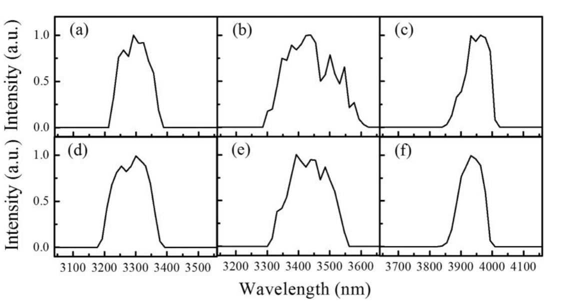

Fig. 2. Typical spectra of mid-IR pulses (a)–(c) generated by the femtosecond OPA and (d)–(f) amplified by the OPCPA.

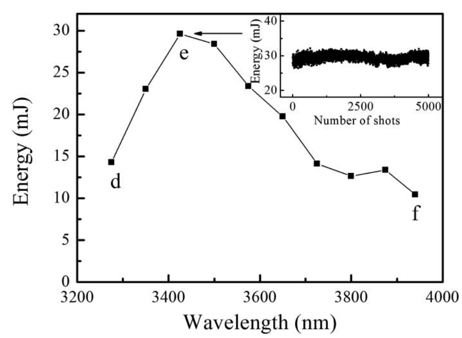

Fig. 3. Measured chirped-pulse energies at different wavelengths. Spectra of pulses at (d) 3275 nm, (e) 3425 nm, and (f) 3940 nm are shown in Figs. 2(d)–2(f), respectively. Inset: Pulse-energy display over 5000 shots.

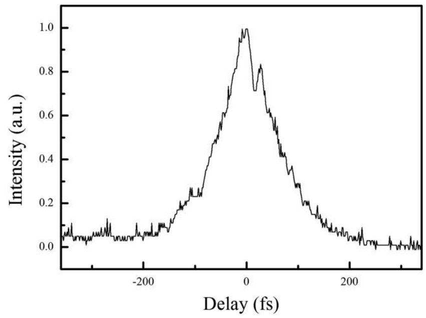

Fig. 4. Measured single-shot cross-correlation trace for mid-IR pulses at 3425 nm.

In the experiment, both the pulse stretcher and compressor were designed for mid-IR pulses, which is crucial for mid-IR dispersion compensation. The calculated residual third-order dispersion (TOD) in our system was only -1.6×10^4 fs^3 that had little affect on the pulse with a duration ~100 fs, while the TOD in the case using a stretcher at NIR (800 nm) and compressor at mid-IR will be ~3 orders of magnitude larger and necessitates the delicate dispersion-controlling techniques such as grism [13]. Limited by the diffraction efficiency (~84%) of the mid-IR gratings, the maximum pulse energy after compression was ~13.3 mJ at a wavelength of 3425 nm. As shown in Fig. 3, the energy stability at 3425 nm was ~3.3% (rms) and was mainly caused by seed and pump fluctuations (0.8% and 1%, respectively). In addition, the mid-IR laser was 3 times the diffraction limit via measuring the near-field and far-field beam sizes with a variable pinhole.

To measure the pulse duration, we conducted a single-shot intensity cross correlator based on noncollinear sum-frequency generation (SFG) between the mid-IR laser and the Ti:sapphire laser. The SFG signals were recorded by a high-resolution CCD (Coherent, Beamview). A typical correlation trace shows a pulse duration of 111 fs at 3425 nm (Fig. 4). Considering the spectral width of 170 nm (corresponding to a Fourier-limited duration of 101 fs) as shown in Fig. 2(e), the generated mid-IR pulse was close to the Fourier limit with a time-bandwidth product of ~0.48. This agrees well with the control of dispersion as discussed above. Since the probe pulse duration was only ~35 fs, the cross-correlation trace directly shows the mid-IR pulse duration without the need for deconvolution. This also suggests that the mid-IR pulse has a well-shaped profile just like the cross-correlation trace shown in Fig. 4. Therefore, a maximum peak power of 120 GW was deduced from the obtained energy and duration of the compressed pulse at 3425 nm. Finally, we simply address the power scaling of this tunable mid-IR OPCPA system. With an available large aperture (∅100 mm) $LiNbO_3$ crystal (CASTECH) and high energy (20 J) Nd:YAG laser (EKSPLA), it is feasible to generate tunable mid-IR femtosecond pulses at the terawatt power level by our mid-IR OPCPA scheme.

In conclusion, a high power widely tunable mid-IR OPCPA scheme has been experimentally demonstrated. By adopting a tunable mid-IR femtosecond OPA as the seeding source and a single-stage noncollinear OPCPA based on $LiNbO_3$ crystal, a tunable mid-IR output from 3.3 to 3.95 μm has been achieved with a saturated high gain over 4000. The OPCPA system has generated mid-IR femtosecond pulses with a peak power as high as 120 GW and can be readily scaled up to the terawatt level. It will be an ideal laser driving source for generating coherent hard x ray and attosecond pulses.

This work was partially supported by the National Basic Research Program of China (Grant No. 2013CBA01505), and the Natural Science Foundation of China (Grant Nos. 61008017 and 60890202).

References

1. T. Popmintchev, M. C. Chen, P. Arpin, M. M. Murnane, and H. C. Kapteyn, Nat. Photonics **4**, 822 (2010).
2. T. Popmintchev, M. C. Chen, D. Popmintchev, P. Arpin, S. Brown, S. Ališauskas, G. Andriukaitis, T. Balčiunas, O. D. Mücke, A. Pugzlys, A. Baltuška, B. Shim, S. E. Schrauth, A. Gaeta, C. Hernández-García, L. Plaja, A. Becker, A. Jaron-Becker, M. M. Murnane, and H. C. Kapteyn, Science **336**, 1287 (2012).
3. A. Dubietis, G. Jonušauskas, and A. Piskarskas, Opt. Commun. **88**, 437 (1992).
4. I. N. Ross, P. Matousek, M. Towrie, A. J. Langley, and J. L. Collier, Opt. Commun. **144**, 125 (1997).
5. D. Herrmann, L. Veisz, R. Tautz, F. Tavella, K. Schmid, V. Pervak, and F. Krausz, Opt. Lett. **34**, 2459 (2009).
6. O. V. Chekhlov, J. L. Collier, I. N. Ross, P. K. Bates, M. Notley, C. Hernandez-Gomez, W. Shaikh, C. N. Danson, D. Neely, P. Matousek, S. Hancock, and L. Cardoso, Opt. Lett. **31**, 3665 (2006).
7. J. V. Rudd, R. J. Law, T. S. Luk, and S. M. Cameron, Opt. Lett. **30**, 1974 (2005).
8. Z. M. Liao, I. Jovanovic, C. A. Ebbers, Y. T. Fei, and B. Chai, Opt. Lett. **31**, 1277 (2006).
9. Y. P. Deng, A. Schwarz, H. Fattahi, M. Ueffing, X. Gu, M. Ossiander, T. Metzger, V. Pervak, H. Ishizuki, T. Taira, T. Kobayashi, G. Marcus, F. Krausz, R. Kienberger, and N. Karpowicz, Opt. Lett. **37**, 4973 (2012).
10. J. Moses, S.-W. Huang, K.-H. Hong, O. D. Mücke, E. L. Falcão-Filho, A. Benedick, F. Ö. Ilday, A. Dergachev, J. A. Bolger, B. J. Eggleton, and F. X. Kärtner, Opt. Lett. **34**, 1639 (2009).
11. O. Chalus, P. K. Bates, M. Smolarski, and J. Biegert, Opt. Express **17**, 3587 (2009).
12. C. Erny, C. Heese, M. Haag, L. Gallmann, and U. Keller, Opt. Express **17**, 1340 (2009).
13. G. Andriukaitis, T. Balčiūnas, S. Ališauskas, A. Pugžlys, A. Baltuška, T. Popmintchev, M. C. Chen, M. M. Murnane, and H. C. Kapteyn, Opt. Lett. **36**, 2755 (2011).
14. J. Moses, H. Suchowski, and F. X. Kärtner, Opt. Lett. **37**, 1589 (2012).
15. D. Kraemer, M. L. Cowan, R. Z. Hua, K. Franjic, and R. J. D. Miller, J. Opt. Soc. Am. B **24**, 813 (2007).
16. T. Wang, H. Y. Zhu, L. J. Qian, G. Xu, and D. Y. Fan, Opt. Commun. **239**, 397 (2004).